Joint Resource Allocation and Data Offloading for Closed-Loop Controls in Satellite-UAV Networks

Chengleyang Lei[1,2], Wei Feng[1,2], Peng Wei[3], Yunfei Chen[4], Ning Ge[1,2], Shiwen Mao[5]

[1]Department of Electronic Engineering, Tsinghua University, Beijing 100084, China
[2]State Key Laboratory of Space Network and Communications, Tsinghua University, Beijing 100084, China
[3]National Key Laboratory of Science and Technology on Communications,
University of Electronic Science and Technology of China, Chengdu 611731, China
[4]Department of Engineering, University of Durham, DH1 3LE Durham, U.K
[5]Department of Electrical and Computer Engineering, Auburn University, Auburn, AL 36849, USA
Contact e-mail: fengwei@tsinghua.edu.cn

2024 16th International Conference on Wireless Communications and Signal Processing (WCSP) | 979-8-3503-9064-3/24/$31.00 ©2024 IEEE | DOI: 10.1109/WCSP62071.2024.10827253

***Abstract*—To efficiently provide coverage for the machines and robots in remote areas, satellites and unmanned aerial vehicles (UAVs) can be utilized. In such scenarios, UAVs need to integrate different functions to support the control tasks of robots efficiently, while satellites can serve as backhaul to the cloud. To improve the overall performance of the closed-loop control tasks of robots, we jointly optimize the communication and computing resource allocation with data offloading. Specifically, we explore the linear quadratic regulator (LQR) cost to measure the control performance and formulate a sum LQR cost minimization problem. An iterative algorithm is proposed to solve the optimization problem. Simulation results are provided to demonstrate the superiority of the proposed scheme.**

***Index Terms*—Closed-loop control, linear quadratic regulator (LQR), satellite, unmanned aerial vehicle (UAV).**

I. Introduction

The future sixth generation (6G) networks are envisioned to facilitate the operation of machines and robots for their tasks [1]. When serving robots in post-disaster or remote areas where terrestrial infrastructures are unavailable, non-terrestrial infrastructures, such as satellites and unmanned aerial vehicles (UAVs), can be utilized [2], [3]. Due to the limited capabilities of individual robots, extra devices should be deployed on UAVs to assist in task execution. For example, sensors are required to obtain environmental information, computing units are required to process data and formulate robotic actions, and communication modules are required for information exchanges. Therefore, UAVs can integrate sensors, base stations, and mobile edge computing (MEC) servers to efficiently support robots.

Due to the limited capacity of UAVs, the onboard resources are usually constrained [4]. Therefore, UAVs may need satellites to offload a portion of data to the cloud for processing. In such cases, the resource allocation and data offloading strategies should be meticulously designed to maximize resource utilization. In the literature, recent research efforts have focused on improving the communication performance by optimizing the resource allocation and data offloading. For example, Hu *et al.* investigated a UAV-aided MEC system and jointly optimized the UAV trajectory, the ratio of offloading tasks, and the user scheduling to minimize the total delays [5]. Authors in [6] maximized the energy efficiency of a space-air-ground integrated network by optimizing the UAV trajectory and resource allocation. In [7], an MEC-assisted integrated aerial-ground network was investigated considering the malicious jamming attacks, where the semantic computation rate was maximized. The above works are valuable for the satellite-UAV networks. However, most of these works focus on the communication performance only, such as latency or energy efficiency. When serving robots for their tasks, the communication systems are designed to enable control. Therefore, the control performance may be more important than merely optimizing communication performance.

Recently, several works have considered the control performance when designing communication systems. Yang *et al.* [8] optimized the power and time allocation to maximize the ratio of the remaining energy to the linear quadratic regulator (LQR) cost, where the LQR cost is a measure of the control performance. Reference [9] maximized the spectral efficiency of a wireless control system by optimizing the bandwidth and power allocation, while satisfying the control convergence rate requirement. These studies have made significant advances towards control-oriented communication system designs. However, the sensing, communication, and computing components in the system need to be jointly considered, as they cooperate closely to accomplish tasks. Furthermore, MEC should be integrated into the system to reduce the computation delay and enhance the control performance.

Motivated by the above issues, we investigate a satellite-UAV network that serves multiple robots simultaneously. We innovatively propose a closed-loop-oriented system design framework, where we focus on the closed-loop control performance and holistically consider the sensing, communication, computing, and control parameters. We utilize the LQR cost to evaluate the control performance, and formulate an optimization problem to minimize the sum LQR cost by optimizing the communication and computing resource allocation and

979-8-3503-9064-3/24/$31.00 ©2024 IEEE

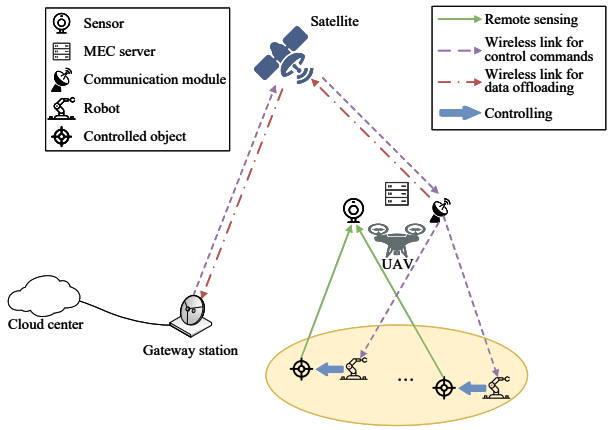

Fig. 1. Illustration of a closed-loop-control-oriented satellite-UAV network.

the data partition. We propose an iterative algorithm to solve this optimization problem. Simulation results are provided to demonstrate the superiority of the proposed scheme over the traditional communication-oriented schemes.

II. System Model and Problem Formulation

As shown in Fig. 1, we consider a satellite-UAV network serving K robots to perform mission-critical tasks. The UAV is equipped with a sensor, an MEC server, and a communication module. Due to the limited computing capability of the UAV, some sensing data is offloaded to the cloud server through the satellite. The satellite links provide backhaul to the powerful cloud center, while the UAV achieves edge capabilities such as sensing, thereby combining the wide coverage of satellites with the on-demand deployment capabilities of UAVs.

During the periodic control process, the onboard sensor monitors the state of the controlled object. Next, the acquired data is analyzed on the servers to generate control commands. The communication module then transmits these commands to robots to guide their actions. The whole process constitutes a closed loop of sensing, communication, computing, and control components, which is referred to as a sensing-communication-computing-control ($\mathbf{SC}^3$) loop. The system enables K $\mathbf{SC}^3$ loops to simultaneously serve K robots.

As described above, different components in the $\mathbf{SC}^3$ loops cooperate closely to accomplish tasks. Considering the coupling of the components, we propose treating the sensing, computing, and communication modules on the UAV as a unified entity. As a center of the task-related information, this entity can be referred to as an edge information hub (EIH) [10]. This allows us to comprehensively consider the influence of the components on the closed-loop performance. Next, we present models of these components in $\mathbf{SC}^3$ loops.

In this paper, we model each robot and its corresponding object as a linear control system. The discrete-time system equation of the k-th control system in cycle t is given by [11]

$$\mathbf{x}_{k,t+1} = \mathbf{A}_k \mathbf{x}_{k,t} + \mathbf{B}_k \mathbf{u}_{k,t} + \mathbf{v}_{k,t}, \tag{1}$$

where t denotes the cycle index, $\mathbf{x}_{k,t} \in \mathbb{R}^{n_k}$ and $\mathbf{u}_{k,t} \in \mathbb{R}^{m_k}$ represent the system state and the control input, n_k and m_k denote their dimensions, $\mathbf{v}_{k,t} \in \mathbb{R}^{n_k}$ denotes the Gaussian noise with mean zero and covariance $\mathbf{\Sigma}_k^{\mathrm{V}}$, and $\mathbf{A}_k$ and $\mathbf{B}_k$ are $n_k \times n_k$ and $n_k \times m_k$ parameter matrices, respectively.

We utilize the LQR cost to evaluate the control performance of the $\mathbf{SC}^3$ loop, which is formulated as [11]

$$l_k \triangleq \lim_{N\to\infty} \mathbb{E}\left[\frac{1}{N}\sum_{t=1}^{N}\left(\mathbf{x}_{k,t}^{\mathrm{T}}\mathbf{Q}_k\mathbf{x}_{k,t} + \mathbf{u}_{k,t}^{\mathrm{T}}\mathbf{R}_k\mathbf{u}_{k,t}\right)\right], \tag{2}$$

where $\mathbf{Q}_k$ and $\mathbf{R}_k$ are semi-positive definite weight matrices. The term $\mathbf{x}_{k,t}^{\mathrm{T}}\mathbf{Q}_k\mathbf{x}_{k,t}$ denotes the deviation of the system from zero state, and the term $\mathbf{u}_{k,t}^{\mathrm{T}}\mathbf{R}_k\mathbf{u}_{k,t}$ represents the control energy consumption. The LQR cost is a comprehensive measure of the state convergence and energy consumption. A small LQR cost indicates a good control performance.

The sensing process is also linear, and the observation equation can be written as

$$\mathbf{y}_{k,t} = \mathbf{C}_k \mathbf{x}_{k,t} + \mathbf{w}_{k,t}, \tag{3}$$

where $\mathbf{y}_{k,t} \in \mathbb{R}^{q_k}$ is the sensing output with q_k denoting its dimension, $\mathbf{C}_k \in \mathbb{R}^{q_k \times n_k}$ is the observation matrix, and $\mathbf{w}_{k,t} \in \mathbb{R}^{q_k}$ is the Gaussian sensing noise with mean zero and covariance $\mathbf{\Sigma}_k^{\mathrm{W}}$.

After the sensing process, the acquired data is analyzed by the computing modules to generate control commands. Due to the limited computing capability of the MEC server, some of these data is transmitted to the cloud server through the satellite. We assume that these data can be arbitrarily split into three parts: the first part is completely processed on the MEC server, the second part is pre-processed on the MEC server to extract semantic features and then sent to the cloud for further processing, and the third part is completely processed on the cloud. The data sizes of these three parts are denoted as $D_{k,1}$, $D_{k,2}$ and $D_{k,3}$ in bits. We have

$$D_{k,1} + D_{k,2} + D_{k,3} = D_k, \tag{4}$$

where D_k is the size of data in the k-th $\mathbf{SC}^3$ loop.

These three parts of data are processed in parallel as data streams. We next analyze the processing time of each data stream. The computing capabilities of the MEC server allocated to the first part and second part of data in $\mathbf{SC}^3$ loop k are denoted as $f_{k,1}$ and $f_{k,2}$, respectively. The backhaul rates from the UAV to the satellite for the second part and third part of data are denoted as $R_{k,2}$ and $R_{k,3}$, respectively. We have the following resource constraints

$$\sum_{k=1}^{K}\left(f_{k,1} + f_{k,2}\right) \le F_{\max}, \tag{5}$$

$$\sum_{k=1}^{K}\left(R_{k,2} + R_{k,3}\right) \le R_{\max}^{\mathrm{U2S}}, \tag{6}$$

where $F_{\max}$ denotes the computing capability of the MEC server, and $R_{\max}^{\mathrm{U2S}}$ denotes the satellite-backhaul rate constraint.

The computation time for the first part of data is

$$T_{k,1}^{\text{comp}} = \frac{\alpha D_{k,1}}{f_{k,1}}, \tag{7}$$

where α denotes the number of CPU cycles for processing the first part of data per bit.

Similarly, the time for pre-processing the second part of data is formulated as

$$T_{k,2}^{\text{proc}} = \frac{\beta D_{k,2}}{f_{k,2}}, \tag{8}$$

where β denotes the number of CPU cycles for pre-processing the second part of data per bit. We assume that the semantic compression ratio of the features-extracting process is ρ, i.e., $\rho D_{k,2}$-bits features will be sent to the cloud server. The transmission latency from the UAV to satellite is

$$T_{k,2}^{\text{trans}} = \frac{\rho D_{k,2}}{R_{k,2}}. \tag{9}$$

We assume that the downlink transmission latency from the satellite to the cloud and the computation time on the cloud server are negligible compared with $T_{k,2}^{\text{trans}}$ and $T_{k,2}^{\text{proc}}$, due to the typically large downlink transmission data rate and computing capability of the cloud. In addition, since the output data size is much smaller than the input data size, the transmission latency of the output data is also assumed negligible. In this case, the overall processing time of the second part of data is

$$T_{k,2}^{\text{comp}} = \begin{cases} 0, & \text{if } D_{k,2} = 0, \\ \max\left\{T_{k,2}^{\text{proc}}, T_{k,2}^{\text{trans}}\right\} + 4\tau, & \text{if } D_{k,2} > 0, \end{cases} \tag{10}$$

where τ is the propagation latency between the ground and the satellite. Since the pre-processing and transmission processes are in parallel, we consider the maximum of these times as the overall latency.

Similarly, the time for processing the third part of data can be calculated by

$$T_{k,3}^{\text{comp}} = \begin{cases} 0, & \text{if } D_{k,3} = 0, \\ \dfrac{D_{k,3}}{R_{k,3}} + 4\tau, & \text{if } D_{k,3} > 0. \end{cases} \tag{11}$$

Based on the above analysis, the overall computation time is the maximum time for processing the three parts of data as

$$T_k^{\text{comp}} = \max\left\{T_{k,1}^{\text{comp}}, T_{k,2}^{\text{comp}}, T_{k,3}^{\text{comp}}\right\}. \tag{12}$$

After analyzing the data, control commands will be transmitted to the corresponding robots. The commands are transmitted through orthogonal (e.g., in frequency) channels, so we assume that there is no interference among the links. The data rate from the UAV to robot k can be calculated as

$$R_k^{\text{U2G}}(p_k) = \log_2\left(1 + \frac{g_k p_k}{\sigma^2}\right), \tag{13}$$

where p_k denotes the transmit power of $\mathbf{SC}^3$ loop k, g_k represents the channel power gain, and σ^2 denotes the channel noise power. The channels between the UAV and robots are assumed to be dominated by line-of-sight (LoS) links, so we have $g_k = \frac{\gamma_0}{d_k^2}$, where d_k denotes the distance between the UAV and robot k, and γ_0 is the reference channel power gain at a distance of one meter. We have

$$\sum_{k=1}^{K} p_k \le P_{\max}, \tag{14}$$

where $P_{\max}$ represents the transmit power constraint.

Denoting the transmission time for the control commands as T_k^{commu}, we have

$$T_k^{\text{comp}} + T_k^{\text{commu}} \le T_k, \tag{15}$$

where T_k is the time resource reserved for the computing and communication processes in each cycle of $\mathbf{SC}^3$ loop k.

To improve the control performance, we optimize the resource allocation and data offloading. Next, we establish the relationship between the control performance and the communication capability. According to [11], to achieve a certain LQR cost l_k, the average data throughput transmitted through channel k per cycle must satisfy the following constraint

$$BT_k^{\text{commu}} R_k^{\text{U2G}}(p_k) \ge \overline{e}_k(l_k), \tag{16}$$

where the left side of (16) denotes the information entropy transmitted per cycle, and

$$\overline{e}_k(l_k) \triangleq h_k + \frac{n_k}{2}\log_2\left(1 + \frac{n_k|\det \mathbf{N}_k\mathbf{M}_k|^{\frac{1}{n_k}}}{l_k - l_{\min,k}}\right) \tag{17}$$

denotes the minimum entropy to achieve the LQR cost l_k, $h_k \triangleq \log_2|\det \mathbf{A}_k|$ is the intrinsic entropy rate of object k, $l_{\min,k} = \text{tr}\left(\mathbf{\Sigma}_k^{\text{V}}\mathbf{S}_k\right) + \text{tr}\left(\mathbf{\Sigma}_k\mathbf{A}_k^{\text{T}}\mathbf{M}_k\mathbf{A}_k\right)$ denotes the lower bound of the LQR cost, $\mathbf{N}_k$, $\mathbf{M}_k$ and $\mathbf{S}_k$ are the solutions to the matrix equations shown in [11], which are related to the control parameters, i.e., $\mathbf{A}_k$, $\mathbf{B}_k$, $\mathbf{R}_k$, $\mathbf{Q}_k$, $\mathbf{\Sigma}_k^{\text{V}}$, and $\mathbf{\Sigma}_k^{\text{W}}$.

Using (16), we minimize the sum LQR costs by jointly optimizing the transmit power $\mathbf{p} = \{p_k\}$, the computing capability $\mathbf{f} = \{f_{k,1}, f_{k,2}\}$, the satellite transmission rate $\mathbf{R} = \{R_{k,2}, R_{k,3}\}$, and the data partition $\mathbf{D} = \{D_{k,1}, D_{k,2}, D_{k,3}\}$. The optimization problem is formulated as

$$\min_{\mathbf{p},\mathbf{f},\mathbf{R},\mathbf{D}} \quad \sum_{k=1}^{K} l_k \tag{18a}$$

$$\textit{s.t.} \quad \sum_{k=1}^{K} p_k \le P_{\max}, \tag{18b}$$

$$D_{k,1} + D_{k,2} + D_{k,3} = D_k, \quad k = 1, 2, \cdots, K, \tag{18c}$$

$$\sum_{k=1}^{K} (f_{k,1} + f_{k,2}) \le F_{\max}, \tag{18d}$$

$$\sum_{k=1}^{K} (R_{k,2} + R_{k,3}) \le R_{\max}^{\text{U2S}}, \tag{18e}$$

$$T_k^{\text{comp}} + T_k^{\text{commu}} \le T_k, \quad k = 1, 2, \cdots, K, \tag{18f}$$

$$BT_k^{\text{commu}} R_k^{\text{U2G}}(p_k) \ge \overline{e}_k(l_k), \ k = 1, 2, \cdots, K. \tag{18g}$$

Problem (18) is difficult to solve due to the non-convex and

non-continuous expression of T_k^{comp} as in (12). Next, we will recast this problem to a more tractable form and propose an iterative algorithm to solve it.

III. Joint Resource Allocation and Data Offloading

In this section, we will solve the optimization problem (18) by proposing an iterative algorithm based on the successive convex approximation (SCA) method.

A. Problem Simplification

From (18), we can find that the data partition parameters of each $\mathbf{SC}^3$ loop will be decoupled if the computing capability allocation and satellite-backhaul rate allocation are given. As l_k is monotonically decreasing with the transmission time T_k^{commu}, the optimal offloading scheme to minimize the LQR cost also minimizes the computing time. Therefore, the optimal data partition scheme in $\mathbf{SC}^3$ loop k, given the computing capability allocation and satellite-backhaul rate allocation, can be obtained by solving the following optimization problem

$$\min_{\mathbf{D}_k,\mathbf{f}_k,\mathbf{R}_k} \quad \max\left\{T_{k,1}^{\text{comp}}, T_{k,2}^{\text{comp}}, T_{k,3}^{\text{comp}}\right\} \tag{19a}$$

$$s.t. \quad D_{k,1}+D_{k,2}+D_{k,3} = D_k, \tag{19b}$$

$$f_{k,1} + f_{k,2} \le f_k, \tag{19c}$$

$$R_{k,2} + R_{k,3} \le R_k, \tag{19d}$$

where f_k and R_k denote the computing capability and satellite-backhaul rate allocated to $\mathbf{SC}^3$ loop k, respectively, and the variable vectors to be optimized are $\mathbf{D}_k = [D_{k,1}, D_{k,2}, D_{k,3}]$, $\mathbf{f}_k = [f_{k,1}, f_{k,2}]$ and $\mathbf{R}_k = [R_{k,2}, R_{k,3}]$.

Once the problem (19) is solved, the optimal resource allocation can be obtained via the following problem

$$\min_{\mathbf{p},\mathbf{f}',\mathbf{R}',\mathbf{l}} \quad \sum_{k=1}^{K} l_k \tag{20a}$$

$$s.t. \quad \sum_{k=1}^{K} p_k \le P_{\max}, \tag{20b}$$

$$\sum_{k=1}^{K} f_k \le F_{\max}, \tag{20c}$$

$$\sum_{k=1}^{K} R_k \le R_{\max}^{\text{U2S}}, \tag{20d}$$

$$T_k^{\text{comp},*}(f_k, R_k) + T_k^{\text{commu}} \le T_k, \ k = 1, 2, \cdots, K, \tag{20e}$$

$$BT_k^{\text{commu}} R_k^{\text{U2G}}(p_k) \ge \overline{e}_k(l_k), \ k = 1, 2, \cdots, K, \tag{20f}$$

where $\mathbf{l} = [l_1, l_2, \cdots, l_K]$, $\mathbf{f}' = \{f_k\}$ and $\mathbf{R}' = \{R_k\}$. The function $T_k^{\text{comp},*}(f_k, R_k)$ denotes the minimal computation time of loop k when f_k and R_k are given, which is the optimal value of the objective function of (19).

To solve (20), we give the closed-form expression of $T_k^{\text{comp},*}(f_k, R_k)$ by solving (19) in the following proposition.

Proposition 1: *$T_k^{comp,*}(f_k, R_k)$ is given by the piece-wise function shown in* (21) *on the next page.*

Proof: If $f_k \ge \frac{\alpha D_k}{4\tau}$, we have $\frac{\alpha D_k}{f_k} < 4\tau$, indicating that the time to process all the data locally will be less than the propagation delay 4τ. In such a case, all the data should be processed on the MEC, and we have $T_k^{\text{comp}} = T_{k,1}^{\text{comp}} = \frac{\alpha D_k}{f_k}$.

On the contrary, if $f_k < \frac{\alpha D_k}{4\tau}$, we have

$$T_{k,1}^{\text{comp}} = T_{k,2}^{\text{comp}} = T_{k,3}^{\text{comp}}, \tag{22}$$

$$T_{k,2}^{\text{proc}} = T_{k,2}^{\text{trans}}. \tag{23}$$

Otherwise, we can adjust the data partition or the resource allocation within $\mathbf{SC}^3$ loop k, to keep the overall computing time non-increasing. In addition, as the latency is non-increasing with respect to $f_{k,1}$, $f_{k,2}$, $R_{k,1}$ and $R_{k,2}$, we have $f_{k,1} + f_{k,2} = f_k$ and $R_{k,2} + R_{k,3} = R_k$. Based on the above equations, we have $f_{k,1} = f_k - f_{k,2}$, $R_{k,2} = \frac{\rho}{\beta} f_{k,2}$, and $R_{k,3} = R_k - \frac{\rho}{\beta} f_{k,2}$. Substituting these variables into (19b) and (22), we can formulate T_k^{comp} as

$$T_k^{\text{comp}} = \frac{\alpha\beta D_k - 4\beta\tau f_k + 4\beta\tau f_{k,2}}{(\alpha - \alpha\rho - \beta) f_{k,2} + \beta f_k + \alpha\beta R_k} + 4\tau. \tag{24}$$

In (24), we formulate T_k^{comp} as a fractional linear function of $f_{k,2}$. Therefore, T_k^{comp} is monotonic with respect to $f_{k,2}$. If $4\beta\tau R_k - (\alpha - \alpha\rho - \beta) D_k + 4(1-\rho)\tau f_k \ge 0$, it can be proved that T_k^{comp} is increasing with respect to $f_{k,2}$. In such case, $f_{k,2} = 0$ must hold to minimize T_k^{comp}, and we have

$$T_k^{\text{comp}} = \frac{\alpha D_k - 4\tau f_k}{f_k + \alpha R_k} + 4\tau. \tag{25}$$

Similarly, if $4\beta\tau R_k - (\alpha - \alpha\rho - \beta) D_k + 4(1-\rho)\tau f_k \le 0$, $f_{k,2}$ should be as large as possible. With the constraints $f_{k,1} \ge 0$ and $R_{k,3} \ge 0$, we can obtain the optimal value of $f_{k,2}$, and calculate the corresponding computing time, which completes the proof. More detailed proof can be found in our extended paper [10]. □

B. Iterative Algorithm to solve (20)

Although we recast the original problem (18) to a more tractable form (20), it is still difficult to solve it as it is a non-convex optimization problem. In this subsection, we propose an iterative algorithm to solve (20) based on the SCA method.

First, in order to address the non-convexity of constraint (20f), we include the communication time $\{T_k^{\text{commu}}\}$ as variables to be optimized, and rewrite (20) as

$$\min_{\mathbf{p},\mathbf{f}',\mathbf{R}',\mathbf{l},\mathbf{T}^{\text{commu}}} \quad \sum_{k=1}^{K} l_k \tag{26a}$$

$$s.t. \quad \sum_{k=1}^{K} p_k \le P_{\max}, \tag{26b}$$

$$\sum_{k=1}^{K} f_k \le F_{\max}, \tag{26c}$$

$$\sum_{k=1}^{K} R_k \le R_{\max}^{\text{U2S}}, \tag{26d}$$

$$T_k^{\text{comp},*}(f_k,R_k)=\begin{cases} T_k^1\left(f_k,R_k\right)\triangleq\dfrac{\beta D_k}{\beta R_k+(1-\rho)\,f_k}+4\tau, \quad \left(f_k,R_k\right)\in\mathcal{S}_1\triangleq\left\{(f,R)\mid 0\le f\le\min\left\{\dfrac{(\alpha-\alpha\rho-\beta)\,D_k-4\beta\tau R}{4\,(1-\rho)\,\tau},\dfrac{\beta R}{\rho}\right\}\right\} \\ T_k^2\left(f_k,R_k\right)\triangleq\dfrac{\rho\alpha D_k-4\rho\tau f_k+4\beta R_k\tau}{\rho f_k+(\alpha-\beta)\,R_k}+4\tau,\ \left(f_k,R_k\right)\in\mathcal{S}_2\triangleq\left\{(f,R)\mid \dfrac{\beta R}{\rho}\le f\le\dfrac{(\alpha-\alpha\rho-\beta)\,D_k-4\beta\tau R}{4\,(1-\rho)\,\tau},R\ge 0\right\} \\ T_k^3\left(f_k,R_k\right)\triangleq\dfrac{\alpha D_k-4\tau f_k}{f_k+\alpha R_k}+4\tau,\ \left(f_k,R_k\right)\in\mathcal{S}_3\triangleq\left\{(f,R)\mid \dfrac{(\alpha-\alpha\rho-\beta)\,D_k-4\beta\tau R}{4\,(1-\rho)\,\tau}\le f\le\dfrac{\alpha D_k}{4\tau},f\ge 0,R\ge 0\right\} \\ T_k^4\left(f_k,R_k\right)\triangleq\dfrac{\alpha D_k}{f_k}, \quad \left(f_k,R_k\right)\in\mathcal{S}_4\triangleq\left\{(f,R)\mid f\ge\dfrac{\alpha D_k}{4\tau},R\ge 0\right\}\end{cases} \tag{21}$$

$$\overline{T}_k^{\text{comp},*}\left(f_k,R_k|f_{k0},R_{k0}\right)=\begin{cases}\max\left\{T_k^1\left(f_k,R_k\right),\overline{T}_k^2\left(f_k,R_k|f_{k0},R_{k0}\right)\right\}, & \left(f_{k0},R_{k0}\right)\in\mathcal{S}_1\cup\mathcal{S}_2\\ \overline{T}_k^3\left(f_k,R_k|f_{k0},R_{k0}\right), & \left(f_{k0},R_{k0}\right)\in\mathcal{S}_3\\ T_k^4\left(f_k,R_k\right), & \left(f_{k0},R_{k0}\right)\in\mathcal{S}_4\end{cases} \tag{29}$$

$$T_k^{\text{comp},*}\left(f_k,R_k\right)+T_k^{\text{commu}}\le T_k,\quad k=1,2,\cdots,K, \tag{26e}$$

$$BR_k^{\text{U2G}}\left(p_k\right)\ge\frac{\overline{e}_k\left(l_k\right)}{T_k^{\text{commu}}},\quad k=1,2,\cdots,K, \tag{26f}$$

where $\mathbf{T}^{\text{commu}}=\{T_k^{\text{commu}}\}$. It can be shown that the function $\frac{\overline{e}_k(l_k)}{T_k^{\text{commu}}}$ is convex with respect to (l_k,T_k^{commu}). Therefore, constraint (26f) describes a convex set. Next, we handle the non-convexity of the function $T_k^{\text{comp},*}(f_k,R_k)$ in (26e).

To solve (26), we propose an iterative algorithm based on the SCA method. First, we introduce the following proposition in order to approximate $T_k^{\text{comp},*}\left(f_k,R_k\right)$.

Proposition 2: *For any $x>0$, $y>0$, $x_0>0$ and $y_0>0$, we have the following inequality*

$$\frac{1}{xy}\ge\frac{1}{x_0y_0}\left(3-\frac{x}{x_0}-\frac{y}{y_0}\right). \tag{27}$$

The equality holds when $x=x_0$ and $y=y_0$.

Proof: Using the Hessian matrix, it can be shown that $1/xy$ is convex with $x>0$, $y>0$. The inequality in (27) can be obtained immediately through the first-order condition of convex functions [12, Section 3.1.3]. □

Substituting $x=1/u, y=au+bv, x_0=1/u_0$, and $y_0=au_0+bv_0$ into (27), we have

$$\frac{u}{au+bv}\ge\frac{u_0}{au_0+bv_0}\left(3-\frac{u_0}{u}-\frac{au+bv}{au_0+bv_0}\right), \tag{28}$$

where $a>0$, $b>0$, $u>0$, and $v>0$. Based on (28), we approximate $T_k^{\text{comp},*}(f_k,R_k)$ by a convex function $\overline{T}_k^{\text{comp},*}\left(f_k,R_k|f_{k0},R_{k0}\right)$, which is formulated as (29) at the top of this page. The functions $\overline{T}_k^2\left(f_k,R_k|f_{k0},R_{k0}\right)$ and $\overline{T}_k^3\left(f_{k0},R_{k0}\right)$ in (29) are two functions that approximate $T_k^2\left(f_k,R_k\right)$ and $T_k^3\left(f_k,R_k\right)$ based on (28), respectively, as shown in (30) and (32) on the next page.

The following proposition gives the properties of $\overline{T}_k^{\text{comp},*}$.

Proposition 3: *The function $\overline{T}_k^{\text{comp},*}\left(f_k,R_k|f_{k0},R_{k0}\right)$ shown in* (29) *is convex, and satisfies the following inequality*

$$\overline{T}_k^{\text{comp},*}\left(f_k,R_k|\ f_{k0},R_{k0}\right)\ge T_k^{\text{comp},*}\left(f_k,R_k\right), \tag{34}$$

where f_{k0} and R_{k0} are non-negative constants, and the equality holds when $f_k=f_{k0}$, and $R_k=R_{k0}$.

Proof: First, as T_k^1, $\overline{T}_k^2$, $\overline{T}_k^3$ and T_k^4 are reciprocal functions of the linear combination of f_k and R_k, we can obtain the convexity of $\overline{T}_k^{\text{comp},*}\left(f_k,R_k|f_{k0},R_{k0}\right)$.

Next, by comparing the values of $T_k^i\left(f_k,R_k\right)$ for $i\in[1,2,3,4]$, we can establish the relationship among the four functions when (f_k,R_k) is in different regions as

$$T_k^4\left(f_k,R_k\right)>T_k^3\left(f_k,R_k\right)>T_k^1\left(f_k,R_k\right),\ \left(f_k,R_k\right)\in\mathcal{S}_1, \tag{35a}$$
$$T_k^4\left(f_k,R_k\right)>T_k^3\left(f_k,R_k\right)\ge T_k^2\left(f_k,R_k\right),\ \left(f_k,R_k\right)\in\mathcal{S}_2, \tag{35b}$$
$$T_k^1\left(f_k,R_k\right)\ge T_k^2\left(f_k,R_k\right)\ge T_k^3\left(f_k,R_k\right),\ \left(f_k,R_k\right)\in\mathcal{S}_3, \tag{35c}$$
$$T_k^4\left(f_k,R_k\right)\ge T_k^3\left(f_k,R_k\right),\ \left(f_k,R_k\right)\in\mathcal{S}_3, \tag{35d}$$
$$T_k^2\left(f_k,R_k\right)\ge T_k^3\left(f_k,R_k\right)>T_k^4\left(f_k,R_k\right),\ \left(f_k,R_k\right)\in\mathcal{S}_4. \tag{35e}$$

Therefore, if $(f_{k0},R_{k0})\in\mathcal{S}_1\cup\mathcal{S}_2$, we have

$$\overline{T}_k^{\text{comp},*}\left(f_k,R_k|\ f_{k0},R_{k0}\right) \tag{36a}$$
$$=\max\left\{T_k^1\left(f_k,R_k\right),\overline{T}_k^2\left(f_k,R_k|f_{k0},R_{k0}\right)\right\} \tag{36b}$$
$$\ge\max\left\{T_k^1\left(f_k,R_k\right),T_k^2\left(f_k,R_k\right)\right\} \tag{36c}$$
$$\ge T_k^{\text{comp},*}\left(f_k,R_k\right), \tag{36d}$$

where (36d) can be obtained from (35) by examining the cases separately where (f_k,R_k) belongs to different regions.

Following a similar procedure, it can be proven that $\overline{T}_k^{\text{comp},*}\left(f_k,R_k|\ f_{k0},R_{k0}\right)\ge T_k^{\text{comp},*}\left(f_k,R_k\right)$ when $(f_{k0},R_{k0})\in\mathcal{S}_3$ and $(f_{k0},R_{k0})\in\mathcal{S}_4$.

Finally, since $\overline{T}_k^2\left(f_{k0},R_{k0}|f_{k0},R_{k0}\right)=T_k^2\left(f_{k0},R_{k0}\right)$ and $\overline{T}_k^3\left(f_{k0},R_{k0}|f_{k0},R_{k0}\right)=T_k^3\left(f_{k0},R_{k0}\right)$, the equality condition in **Proposition 3** is obtained. □

By approximating $T_k^{\text{comp},*}(f_k,R_k)$ to $\overline{T}_k^{\text{comp},*}\left(f_k,R_k|f_{k0},R_{k0}\right)$, the approximate optimization

$$\overline{T}_k^2\left(f_k,R_k|f_{k0},R_{k0}\right)\triangleq\frac{\rho\alpha D_k}{\rho f_k+(\alpha-\beta)R_k}+4\frac{\alpha\tau}{\alpha-\beta}-\frac{\frac{4\rho\alpha\tau}{\alpha-\beta}f_{k0}}{\rho f_{k0}+(\alpha-\beta)R_{k0}}\left[3-\frac{f_{k0}}{f_k}-\frac{\rho f_k+(\alpha-\beta)R_k}{\rho f_{k0}+(\alpha-\beta)R_{k0}}\right] \tag{30}$$

$$\geq\frac{\rho\alpha D_k}{\rho f_k+(\alpha-\beta)R_k}+4\frac{\alpha\tau}{\alpha-\beta}-\frac{\frac{4\rho\alpha\tau}{\alpha-\beta}f_k}{\rho f_k+(\alpha-\beta)R_k}=T_k^2\left(f_k,R_k\right) \tag{31}$$

$$\overline{T}_k^3\left(f_k,R_k|f_{k0},R_{k0}\right)\triangleq\frac{\alpha D_k}{f_k+\alpha R_k}+4\tau-\frac{4\tau f_{k0}}{f_{k0}+\alpha R_{k0}}\left[3-\frac{f_{k0}}{f_k}-\frac{f_k+\alpha R_k}{f_{k0}+\alpha R_{k0}}\right] \tag{32}$$

$$\geq\frac{\alpha D_k}{f_k+\alpha R_k}+4\tau-\frac{4\tau f_k}{f_k+\alpha R_k}=T_k^3\left(f_k,R_k\right) \tag{33}$$

Algorithm 1: Iterative algorithm for solving problem (20)

Input : System parameters $P_{\max}$, $F_{\max}$, $R_{\max}$, etc; the convergence tolerance ϵ.

Initialization: Calculate a feasible $\mathbf{f}'^0$ and $\mathbf{R}'^0$ based on (20c) and (20d), and set $i=0$

repeat

  Set $i=i+1$;

  Update $\mathbf{p}^i$, $\mathbf{f}'^i$ and $\mathbf{R}'^i$ by solving (37), denote the value of the objective function as L^t;

until $\frac{L^{i-1}-L^i}{L^{i-1}}<\epsilon$;

Output : The optimal resource allocation $\mathbf{p}^i$, $\mathbf{f}'^i$, $\mathbf{R}'^i$, and the sum LQR cost L^i.

problem of (26) is formulated as

$$\min_{\mathbf{p},\mathbf{f}',\mathbf{R}',\mathbf{l},\mathbf{T}^{\text{commu}}}\ \sum_{k=1}^{K}l_k \tag{37a}$$

$$s.t.\ \overline{T}_k^{\text{comp},*}\left(f_k,R_k|f_k^{(i-1)},R_k^{(i-1)}\right)+T_k^{\text{commu}}\leq T_k,\quad k=1,2,\cdots,K, \tag{37b}$$

$$(26b)-(26d),(26f), \tag{37c}$$

where i is the iteration index, and $f_k^{(i-1)}$ and $R_k^{(i-1)}$ denote the solutions in the $(i-1)$-th iteration. As $\overline{T}_k^{\text{comp},*}\left(f_k,R_k|f_{k0},R_{k0}\right)$ is a convex function, problem (37) is convex, which can be solved efficiently by convex optimization tools [12].

By solving (37) iteratively, **Algorithm 1** is proposed to solve (20). Denoting the optimal solution to problem (37) in the i-th iteration as $\left(\mathbf{p}^i,\mathbf{f}'^i,\mathbf{R}'^i,\mathbf{l}^i,\mathbf{T}^{\text{commu},i}\right)$, we have

$$\overline{T}_k^{\text{comp},*}\left(f_k^{(i-1)},R_k^{(i-1)}|f_k^{(i-1)},R_k^{(i-1)}\right)+T_k^{\text{commu}} \tag{38a}$$

$$=T_k^{\text{comp},*}\left(f_k^{(i-1)},R_k^{(i-1)}\right)+T_k^{\text{commu}} \tag{38b}$$

$$\leq\overline{T}_k^{\text{comp},*}\left(f_k^{(i-1)},R_k^{(i-1)}|f_k^{(i-2)},R_k^{(i-2)}\right)+T_k^{\text{commu}} \tag{38c}$$

$$\leq T_k, \tag{38d}$$

where (38c) follows from (34), and (38d) holds because $\mathbf{f}'^{i-1}$ and $\mathbf{R}'^{i-1}$ are the optimal solutions to (37) in the $(i-1)$-th iteration and should satisfy the constraint (37b). Therefore, $\left(\mathbf{p}^{(i-1)},\mathbf{f}'^{(i-1)},\mathbf{R}'^{(i-1)},\mathbf{l}^{(i-1)},\mathbf{T}^{\text{commu},(i-1)}\right)$ is also feasible to the optimization problem (37) in the i-th iteration, indicating that the objective function is non-increasing during the iteration. Therefore, **Algorithm 1** converges.

Next, we analyze the computational complexity of **Algorithm 1**. Optimization problem (37) is a convex problem, which can be solved by interior point method with the complexity of $\mathcal{O}\left(K^{3.5}\log\left(1/\epsilon_0\right)\right)$, where ϵ_0 is the solution accuracy [13]. Therefore, the computational complexity of the proposed algorithm is $\mathcal{O}\left(I_1K^{3.5}\log\left(1/\epsilon_0\right)\right)$, where I_1 is the iteration number of **Algorithm 1**.

IV. Simulation Results

In this section, simulation results are provided to evaluate the proposed joint resource allocation and data offloading scheme. The number of robots is set as $K=5$. The robots are assumed to be randomly distributed in a circular area with a radius of 5000 m, where the UAV is at the center of the circular area with a height of 100 m. We set $B=5$ kHz, $\tau=5$ ms, $\beta_0=-60$ dB, and $\sigma^2=-110$ dBm [14]. For the computing parameters, we set $D_k=300$ Mb, $\rho=0.2$, $\alpha=100$ CPU cycles/bit, and $\beta=50$ CPU cycles/bit. Unless otherwise specified, the resource constraints are set as $T_k=70$ ms, $F_{\max}=5$ GHz, $P_{\max}=10$ dBW and $R_{\max}^{\text{U2S}}=50$ Mbps.

For the control parameters, the state matrices $\mathbf{A}_k$ are assumed to be 50×50 diagonal matrices with diagonal elements randomly selected in $[-10,10]$. The covariance matrices of the control system noise and sensing noise are $\mathbf{\Sigma}_k^{\text{V}}=\sigma_{\text{V},k}^2\times\mathbf{I}_n$ and $\mathbf{\Sigma}_k^{\text{W}}=\sigma_{\text{W},k}^2\times\mathbf{I}_n$, with $n=50$, $\sigma_{\text{V},k}^2=\sigma_{\text{V}}^2=0.01$, and $\sigma_{\text{W},k}^2=\sigma_{\text{W}}^2=0.001$. The observation matrices and the LQR weight matrices are set as $\mathbf{C}_k=\mathbf{I}_n$, $\mathbf{Q}_k=\mathbf{I}_n$, $\mathbf{R}_k=\mathbf{0}$.

To evaluate the proposed algorithm, we compare it with the following benchmark schemes.

- Closed-loop-oriented power allocation: optimizing transmit power allocation to minimize the sum LQR cost as in [15], where the computing capability and the satellite-backhaul rate are allocated equally to the loops.
- Communication-oriented scheme: optimizing the computing capability allocation to minimize the sum computation time [16], where the satellite-backhaul rate is allocated equally to the loops, then the transmit power allocation is optimized to maximize the data throughput.

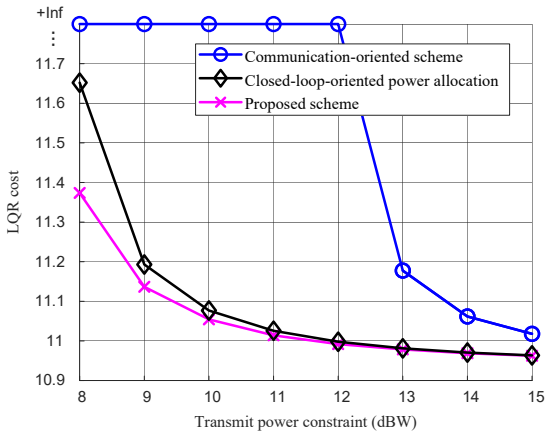

Fig. 2. LQR cost achieved by different schemes, varying with the transmit power constraint.

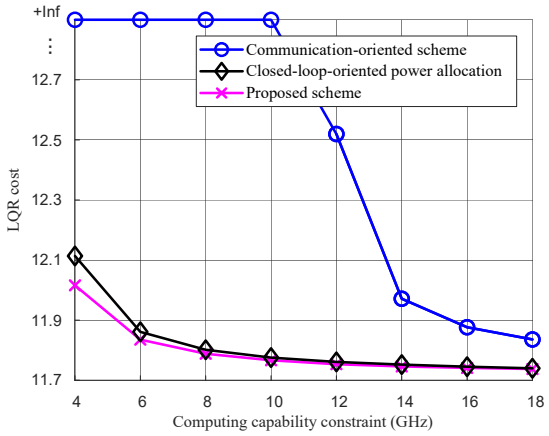

Fig. 3. LQR cost achieved by different schemes, varying with the computing capability constraint.

Fig. 2 shows the LQR cost achieved by the three schemes under different transmit power constraints. Note that the control system with the communication-oriented scheme is unstable when the power constraint is lower than 12 dBW, so the LQR cost is infinite. It is seen that the LQR cost decreases with increased power constraint. This is because more exact control commands can be transmitted as the transmit power increases, leading to an improved control performance. In addition, the proposed scheme achieves the lowest LQR cost among the three schemes, showing its superiority.

In Fig. 3, we show the LQR cost under different computing capability constraints. We can see that the proposed scheme achieves lower LQR cost than the benchmark schemes. Similar to Fig. 2, it is shown that the LQR cost decreases with increased $F_{\max}$, as the time available for communication increases with the increase of the computing capability.

V. Conclusion

In this paper, we investigated a satellite-UAV network serving multiple robots for control tasks. In order to improve the overall performance of the tasks, we formulated a sum LQR cost minimization problem by jointly optimizing resource allocation and data offloading. We recast the problem and proposed an iterative algorithm to solve it. Simulation results demonstrated the superiority of the proposed scheme.

Acknowledgment

This work was supported in part by the National Natural Science Foundation of China under Grant U22A2002 and Grant 62341110, in part by the National Key Research and Development Program of China under Grant 2020YFA0711301, in part by the Suzhou Science and Technology Project, and in part by the FAW Jiefang Automotive Co., Ltd.

References

[1] M. Giordani, M. Polese, M. Mezzavilla, S. Rangan and M. Zorzi, "Toward 6G networks: Use cases and technologies," *IEEE Commun. Mag.*, vol. 58, no. 3, pp. 55-61, Mar. 2020.

[2] W. Feng, Y. Wang, Y. Chen, N. Ge, and C.-X. Wang, "Structured satellite-UAV-terrestrial networks for 6G Internet of Things," *IEEE Netw.*, vol. 38, no. 4, pp. 48-54, Jul. 2024.

[3] C. Zeng, J. -B. Wang, C. Ding, M. Lin and J. Wang, "MIMO unmanned surface vessels enabled maritime wireless network coexisting with satellite network: Beamforming and trajectory design," *IEEE Trans. Commun.*, vol. 71, no. 1, pp. 83-100, Jan. 2023.

[4] W. Feng *et al.*, "Radio map-based cognitive satellite-UAV networks towards 6G on-demand coverage," *IEEE Trans. Cogn. Commun. Netw.*, vol. 10, no. 3, pp. 1075-1089, Jun. 2024.

[5] Q. Hu, Y. Cai, G. Yu, Z. Qin, M. Zhao and G. Y. Li, "Joint offloading and trajectory design for UAV-enabled mobile edge computing systems" *IEEE Internet Things J.*, vol. 6, no. 2, pp. 1879-1892, Apr. 2019.

[6] Z. Hu *et al.*, "Joint resources allocation and 3d trajectory optimization for uav-enabled space-air-ground integrated networks," *IEEE Trans. Veh. Technol.*, vol. 72, no. 11, pp. 14214-14229, Nov. 2023.

[7] Y. Sun et al., "Multi-functional RIS-assisted semantic anti-jamming communication and computing in integrated aerial-ground networks," *IEEE J. Sel. Areas Commun.*, early access, 2024.

[8] H. Yang, K. Zhang, K. Zheng and Y. Qian, "Leveraging linear quadratic regulator cost and energy consumption for ultrareliable and low-latency IoT control systems," *IEEE Internet Things J.*, vol. 7, no. 9, pp. 8356-8371, Sep. 2020.

[9] B. Chang, L. Zhang, L. Li, G. Zhao, and Z. Chen, "Optimizing resource allocation in URLLC for real-time wireless control systems," *IEEE Trans. Veh. Tech.*, vol. 68, no. 9, pp. 8916-8927, Sep. 2019.

[10] C. Lei, W. Feng, P. Wei, Y. Chen, N. Ge and S. Mao, "Edge information hub: Orchestrating satellites, UAVs, MEC, sensing and communications for 6G closed-loop controls," *IEEE J. Sel. Areas Commun.*, early access, 2024.

[11] V. Kostina and B. Hassibi, "Rate-cost tradeoffs in control," *IEEE Trans. Auto. Control*, vol. 64, no. 11, pp. 4525-4540, Nov. 2019.

[12] S. Boyd and L. Vandenberghe, *Convex Optimization.* Cambridge, U.K.: Cambridge Univ. Press, 2004.

[13] Y. Du, K. Yang, K. Wang, G. Zhang, Y. Zhao, and D. Chen, "Joint resources and workflow scheduling in UAV-enabled wirelessly-powered MEC for IoT systems," *IEEE Trans. Veh. Technol.*, vol. 68, no. 10, pp. 10187-10200, Oct. 2019.

[14] M. Hua, Y. Wang, Z. Zhang, C. Li, Y. Huang, and L. Yang, "Power-efficient communication in UAV-aided wireless sensor networks," *IEEE Commun. Lett.*, vol. 22, no. 6, pp. 1264-1267, Jun. 2018.

[15] C. Lei *et al.* "Control-oriented power allocation for integrated satellite-UAV networks," *IEEE Wireless Commun. Lett.*, vol. 12, no. 5, pp. 883-887, May 2023.

[16] J. Ren, G. Yu, Y. He and G. Y. Li, "Collaborative cloud and edge computing for latency minimization," *IEEE Trans. Veh. Technol.*, vol. 68, no. 5, pp. 5031-5044, May 2019.